sciendo

POLISH MARITIME RESEARCH 4 (108) 2020 Vol. 27; pp. 17-25
10.2478/pomr-2020-0062

ANALYSIS OF THE DYNAMIC RESPONSE OF OFFSHORE FLOATING WIND POWER PLATFORMS IN WAVES

Li Junlai[1]
Xie Yonghe[2]
Wu Weiguo[1]
Zhang Chi[2]
[1] Wuhan University of Technology, China
[2] ZheJiang Ocean University, China

ABSTRACT

Floating wind power platforms are in constant motion due to waves when deployed at sea. This motion directly affects the stability and safety of the platform. Therefore, it is very important to study the laws governing the platform's dynamic response. In this paper, the dynamic characteristics of an offshore floating wind power platform were analysed under nine different sets of operating conditions using a numerical calculation method. Following this, a scaled 1:50 platform model was tested in a tank. Model tests were carried out with different wave conditions, and dynamic response data for the platform were measured and analysed. The hydrodynamic variation rules of floating wind power generation platform in waves were obtained. Some effective measures for maintain the stability and safety of wind power platforms are put forward that can provide a reference for dynamic stability research and the design of floating wind power platforms in the future.

Keywords: floating wind power platform; dynamic response; inherent laws; numerical calculation; tank test.

INTRODUCTION

At present, efficient equipment for the utilisation of offshore wind energy is being actively developed by scholars all over the world. In order to exploit the available wind energy in the South Baltic Sea region, Polish researchers have focused on exploring the safety and stability of 6 MW offshore wind turbines [7, 8]. At Gdańsk University of Technology, scholars have studied the structural strength and parametric safety analysis of jack-up legs [7]. The stability of floating support structures for offshore wind turbines under towing, settlement and installation at sea has also been studied [8]. Iranian scholars have studied the laws governing the rise and fall of buoys of different shapes in association with offshore floating wind turbines, and the conversion efficiency of wave energy under normal wave conditions [3]. Floating wind power platforms have become the subject of intense research in many countries, and can undergo numerous types of movement when operating under various conditions at sea [1]. These movements will directly affect the safety of the wind power platform and the stability of power generation, and it is therefore very important to study the motion response of floating wind power platforms under the action of waves.

In this paper, a 800 kW floating wind power platform is selected as the research object, and the specific parameters for this platform are presented in Tables 1 and 2. First, the motion response of the floating wind power platform is calculated in the frequency domain using SESAM software (a strength analysis software developed by DNV in 1969), and a model pool test is then conducted to study the movement of the wind power platform under the action of wind and waves.

Tab. 1. Basic parameters of the 800 kW horizontal axis wind motor (full-scale values)

Component name	Specification
Rotor diameter/m	60
Blade /quantity	3
Impeller weight /t	18
Cabin weight /t	36
Engine room size /m	8×4×4

Tab. 2. Main structural dimension parameters of floating foundation (full-scale values)

Component name	Specification /mm	Quantity	Total weight/t	Height of gravitational centre/mm
Water pressure plate	Diameter: 35000 Thickness: 12	3	9.06	6
Buoy	Diameter: 25000 Height: 40000 Thickness: 10	3	739	20000
Cylinder cover	Diameter: 25000 Thickness: 10	3	116	40007
Connection pipe between buoys	Diameter: 2400 Length: 55000 Thickness: 10	6	195	20000
Pillar	Diameter: 6650 Thickness: 10 Length: 45000	1	73.8	42506
Tower	Diameter: 6650 Thickness: 10 Length: 15000	1	24.6	32521
Connection pipe between buoy and tower	Diameter: 2400 Length: 46000 Thickness: 10	6	163	27300

NUMERICAL SIMULATION

Under the action of waves, the wind power platform will be subject to both dynamic and static movements created by the fluid. The equation of motion of a floating body in the frequency domain is [4]:

$$f = [-\omega^2(M + A(\omega)) + i\omega\lambda(\omega) + C + C_m]X \quad (1)$$

where M represents the mass matrix for the floating body, $A(\omega)$ represents the additional mass matrix, $\lambda(\omega)$ represents the damping matrix, C represents the hydrostatic recovery matrix, C_m represents the restoring force matrix of the mooring system, and f represents the wave excitation.

ESTABLISHMENT OF THE FINITE ELEMENT MODEL

The model coordinate system is set up as follows. The origin is at the centre of the projection plane of the floating foundation, where the water-pressure plate is located. The coordinate system is arranged according to the right hand rule: the x-axis is parallel to the central axis of the connecting rod between the central buoy and the main buoy, where the direction from the centre of the supporting buoy towards the main buoy is positive; and the z-axis is along the axis of the tower, where upwards is positive.

SESAM software was used to carry out the modelling. First, the main buoy, the intermediate supporting buoy and the connecting body between the buoy and the tower were established based on the actual geometric size of the wind power platform. The tower was then divided into 10 sections to reflect the linear variation in the wall thickness. The wind turbine was placed on the top of the tower, and the weight of the cabin cover was taken as the weight of the whole cabin. The fan blades were simulated using a circular surface, so that the blades could fully withstand the wind load. Wadam of the HydroD module was used to calculate the motion response. The motion response was calculated using Wadam in Hydro-D module. The structure of the numerical calculation models is shown in Fig. 1.

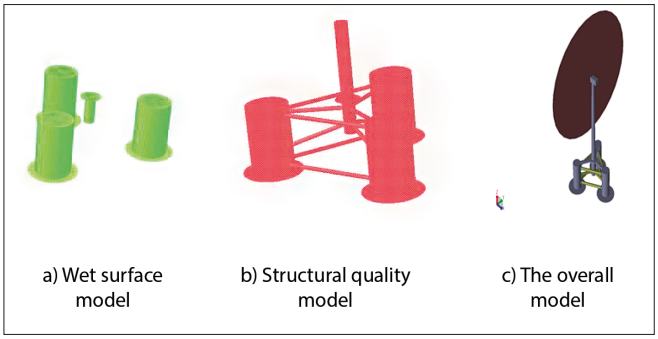

Fig. 1. Numerical calculation model

BOUNDARY CONDITIONS

The boundary constraints of the model were set at the center points of the bottom of the three floating buckets, and different constraint conditions were assigned to these three nodes. Specific boundary conditions were shown in Table 3.

Tab. 3. Boundary conditions

Position	Line displacement constraint		Angular displacement constraint			
	δx	δy	δz	θx	θy	θz
No.1 buoy	limited	limited	limited	related	related	related
No.2 buoy	–	limited	limited	related	related	related
No.3 buoy	–	–	limited	related	related	related

LOAD ANALYSIS

The main load on a floating wind power platform at sea arises from the wind and waves. A detailed analysis is presented below.

Under normal sea conditions, the average pressure on the whole turbine disk is calculated as [10]:

$$P_H = \frac{1}{2}\rho C_{FB} V_r^2 \quad (2)$$

where ρ represents the air density, C_{FB} is a coefficient chosen according to the Bates formula, and V_r is the wind speed. The formula used to calculate the horizontal wind load at the top of the turbine tower is [5]:

$$F_H = P_H A_O = P_H \frac{\pi D^2}{4} \quad (3)$$

The wind load on the tower is calculated as follows [5]:

$$F_{to} = k_1 k_2 a v_t^2 A_w \quad (4)$$

where k_1 represents the shape coefficient of the wind load, k_2 represents the variation coefficient for the air pressure height, a is the wind pressure coefficient, v_t denotes the design wind speed within a given time t, and A_w represents the area of headwind projection for the tower. The MacCamy-Fuchs equation is used to calculate the wave force on large diameter buoys. The formula for calculating the horizontal wave force is as follows [9]:

$$F_H = \int_0^d f_H dz = -\int_0^d \frac{2\rho g H}{k} \frac{chkz}{chkd} A(ka)\sin(\omega t - \alpha)dz \quad (5)$$

where $A(ka)$ is the horizontal amplitude of waves acting on large-scale structure at any height.

The wave load dF on a small-scale member with unit length dz is calculated using the Morison formula [9]:

$$dF = dF_1 + dF_D = \rho \frac{\pi D^2}{4}(C_M \dot{u} - C_A \ddot{x})dz + \frac{1}{2}\rho C_D D|u - \dot{x}|(u - \dot{x})\,dz \quad (6)$$

where dF_1 represents the inertial force per unit length of a small scale member, dF_D is the drag force per unit length on the small-scale components, ρ is the density of seawater, C_M is the inertial coefficient, C_A is the additional mass coefficient, C_D is the drag coefficient, u represents the water particle velocity component perpendicular to the component axis, $\dot{u}$ represents the water particle acceleration component perpendicular to the component axis, $\dot{x}$ represents the velocity component perpendicular to the component axis, and $\ddot{x}$ represents the acceleration component perpendicular to the component axis.

Wind load

The wind load is calculated according to the change in the gradient of the wind pressure coefficient. Since the tower is a cylinder, the coefficient is 0.5, and the wind-affected area is half of the surface area of the tower. The parameters used to calculate the wind load within each gradient range of the tower are shown in Table 4. Eq. (4) is used to calculate the wind load at different heights, and the results are shown in Table 5. The application of wind load is shown in Fig. 2.

Tab. 4. Relative parameters used to calculate wind load [2]

Height range /m	k_2	k_1	Coefficient of wind pressure	Design wind speed /m/s	Upwind projected area/m²
0~2	0.64	0.5	0.613	11	47.1
2~5	0.84	0.5	0.613	11	70.65
5~10	1	0.5	0.613	11	117.75
10~15	1.11	0.5	0.613	11	117.75
15~20	1.18	0.5	0.613	11	117.75
20~20	1.29	0.5	0.613	11	235.5
20~40	1.37	0.5	0.613	11	235.5
40~50	1.43	0.5	0.613	11	117.75

Tab. 5. Numerical values of wind load

Wind load /kN	Wind load per unit area /kN/m²	Application of wind load in numerical calculation /N/mm²
1117.9	23.7	0.024
2200.9	31.2	0.031
4366.9	37.1	0.037
4847.3	41.2	0.041
5153.0	43.8	0.044
11266.7	47.8	0.048
11965.4	50.8	0.051
6244.72	53.0	0.053

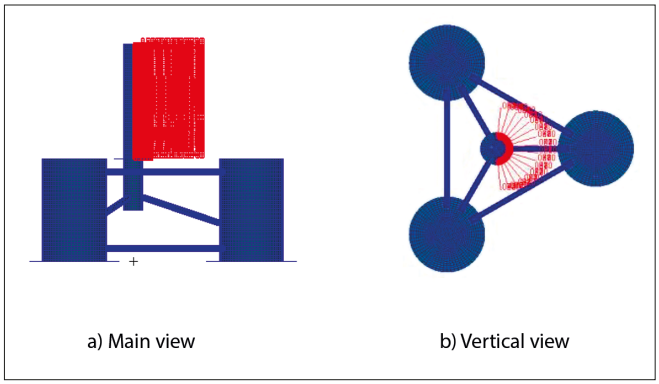

Fig. 2. Application of wind load

Wave load

The effective wavelength and height of the wave load were selected based on the main scale of the floating wind power platform. The specific wave parameters used are shown in Table 6.

Tab. 6. Wave parameters

Angular frequency /rad/s	Wave length /m	Platform length /m	Ratio of wavelength to platform length
1.7	21	105	0.2
1.4	31.5	105	0.3
1.2	42	105	0.4
1.08	52.5	105	0.5
0.99	63	105	0.6
0.92	73.5	105	0.7
0.86	84	105	0.8
0.81	94.5	105	0.9
0.73	115.5	105	1.1
0.7	126	105	1.2
0.67	136.5	105	1.3
0.64	147	105	1.4
0.63	157.5	105	1.5
0.61	168	105	1.6
0.58	178.5	105	1.7
0.57	189	105	1.8
0.56	199.5	105	1.9
0.54	210	105	2

SIMULATED CONDITIONS

To reflect realistic conditions at sea, the rated wind speed for the wind power generation platform was 11 m/s, for a wind and wave direction of 180° and a water depth of 300 m. Nine different conditions of the floating wind power platform were considered, as shown in Table 7.

Tab. 7. Simulated conditions (for a wind speed of 11 m/s)

Serial number (load condition)	Wave height /m	Wave direction /°	Wavelength /m
LC1	3	180	63
LC2	3	180	84
LC3	3	180	105
LC4	3	180	126
LC5	3	180	147
LC6	4	180	105
LC7	5	180	105
LC8	6	180	105
LC9	7	180	105

Tab. 8. Results of the numerical calculations

Serial number	Surge/m	Heave/m	Pitch/°
LC1	1.0	0.19	0.90
LC2	0.88	0.188	0.36
LC3	1.20	0.15	0.40
LC4	1.60	0.09	0.80
LC5	1.80	0.06	0.70
LC6	1.54	0.20	0.53
LC7	1.92	0.25	0.67
LC8	2.31	0.30	0.80
LC9	2.70	0.35	0.94

Tab. 9. Mooring tension at different wavelengths

Wave length /m	Mooring tension/kN		
	No.1 mooring line	No.2 mooring line	No.3 mooring line
63	62.78	57.66	474.06
84	89.69	88.41	589.38
105	49.97	48.69	512.50
126	125.56	103.78	499.69
147	105.06	83.28	448.44

Tab. 10. Mooring tension at different wave heights

Wave length /m	Mooring tension/kN		
	No.1 mooring line	No.2 mooring line	No.3 mooring line
3	53.81	71.75	717.50
4	83.28	89.69	922.50
5	90.97	79.44	1204.38
6	128.13	142.22	1435.00
7	183.22	199.88	1819.38

CALCULATION RESULTS

The results of the finite element calculation are shown in Tables 8–10.

Tab. 11. Conversion relationship between the physical quantities of objects and their model equivalents

Physical quantities	Real objects	Model	Conversion factor
Line scale	L_s	L_m	$L_s/L_m = \lambda$
Linear velocity	V_s	V_m	$V_s/V_m = \lambda^{1/2}$
Linear acceleration	a_s	a_m	$a_s/a_m = 1$
Angle	ϕ_s	ϕ_m	$\phi_s/\phi_m = 1$
Angular velocity	ϕ_s	ϕ_m	$\phi_s/\phi_m = \lambda^{-1/2}$
Action cycle	T_s	T_m	$T_s/T_m = -\lambda^{1/2}$
Inertia moment	I_s	I_m	$I_s/I_m = \gamma\lambda^5$
Force	F_s	F_m	$F_s/F_m = \gamma\lambda^3$

(where λ is the linear scale ratio of the model, and λ is the density ratio of seawater to fresh water)

TANK TEST

TEST MODEL

The model test of the floating wind power platform involves both aerodynamics and hydrodynamics. When creating the test model, it is important to ensure that the blade tip speed ratios (TSRs) of the wind turbine blades are similar, and that the Froude number for the floating base model and the Reynolds number of the platform are similar. The scale of the selected model is 1:50.

The similarity conversion relation between the test model and the actual platform is shown in the following formula. The specific conversion relationship is shown in Table 11.

$$\frac{V_s}{\sqrt{gL_s}} = \frac{V_m}{\sqrt{gL_m}} \tag{7}$$

$$\mathrm{TSR} = \frac{\Omega_s R_s}{U_s} = \frac{\Omega_m R_m}{U_m} \tag{8}$$

where V represents the characteristic velocity in m/s; L represents the characteristic length of the object in m; Ω represents the rotational angular velocity of the impeller in rad/s; R represents the maximum rotation radius of the impeller in m; the subscript s represents real objects; and the subscript m represents the model.

The test model of the floating wind power platform was composed of two parts: the fan and the platform. The main parameters of the model are shown in Tables 12 and 13, and the results are shown in Fig. 3.

Fig. 3 Structure of the test model

Tab. 12. Main parameters of the wind turbine model

Serial number	Name	Specification	Description	Weight /kg
1	Horizontal axial fan	300 W	Head part (consisting mainly of the motor, hub, pressure plate, tail fin and supporting bolts)	32
2	Fan blades	0.6 m	GRP blades, length 0.6 m, three pieces in total	1.5
3	Frequency conversion device	Can provide four levels of speed; It can be controlled according to the test needs	Its weight was negligible	–

Tab. 13. Main parameters of the floating wind power platform model

Serial number	Composition of the test model	Size/mm
1	Diameter of the pressure plate	700
2	Diameter of the float barrel	500
3	Height of the float barrel	800
4	Diameter of the bottom cover of the barrel	500
5	Length of the tube connecting the float barrels	1100
6	Diameter of the pillar	133
7	Height of the pillar	300
8	Diameter of the tower	133
9	Height of the tower	900
10	Length of the tube connecting the float barrel and the tower	920
11	Centre distance of the floating barrel	1600

TEST ENVIRONMENT AND MEASURING EQUIPMENT

The experiment was carried out in the hydrodynamic laboratory of Zhe Jiang Ocean University, and the main scale of the test pool is shown in Table 14 and Fig. 4. At the time of the experiment, the room temperature was 27°C and the water temperature was 25°C.

Fig. 4 Towing tank

Tab. 14. Main scale of pool

Tank parameters	Length/m	Width/m	Height/m
	130	6	3.5

Tab. 15. Other equipment used

Name	No.	Function of equipment
Wave height gauge	1	Measuring the wave parameters
Motion sensor (shown in Figs. 5 and 6)	1	Measuring the longitudinal linear velocity, vertical linear velocity and longitudinal angular displacement of an object
Donghua data collection and analysis system	1	Collecting and analysing experimental data
Digital camera	1	Taking pictures of the experiment

Fig. 5 Tension sensor

Fig. 6 Dip sensor

The measuring equipment used is listed in Table 15.

TESTING PROGRAM

The purpose of this experiment is to study the motion response of the floating wind power platform model under the action of regular waves.

Mooring model simulation

The arrangement of the mooring cables was as follows. Firstly, five weights were tied together to act as mooring points, and a variable pulley was set up at the mooring point. The mooring rope was then passed through the pulley, lifted out of the water, and connected to the pull sensor. It was then towed to the railings of the trailer, and finally, the other end of the mooring line was connected to the bottom of the bucket via the pulley.

In the experiment, three mooring ropes were first arranged using this method. Next, two motion sensors were placed on bucket No. 1 to measure the longitudinal and vertical acceleration of the wind power platform model. A tilt sensor was arranged at the top of the fan to measure the pitching angle of the model platform, as shown in Figs. 7 and 8.

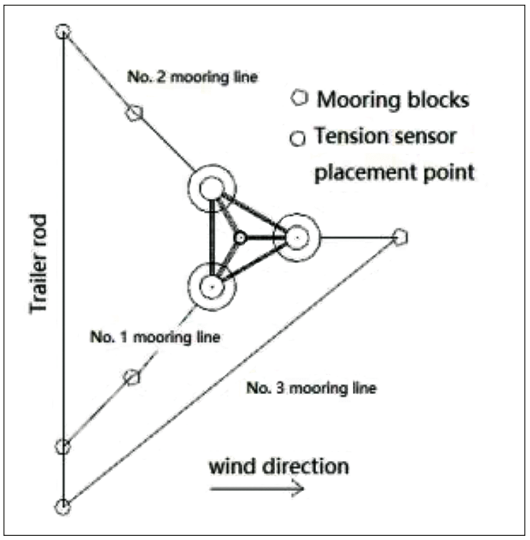

Fig. 7. Mooring model

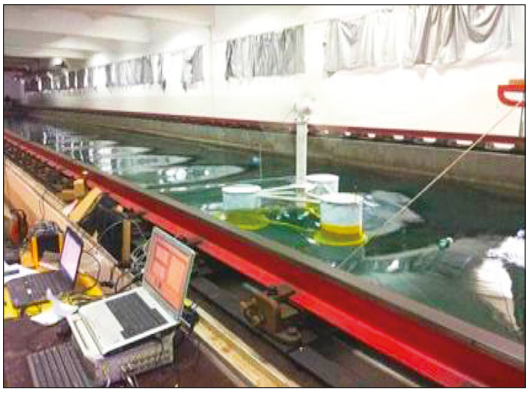

Fig. 8. Test model after debugging

3.3.2 Environmental load simulation

In the tank test, the environmental load mainly consisted of the wave load. Throughout the experiment, the motion response of the fan platform model was measured under different wave conditions, and the research is carried out from two aspects: wave height and wavelength. The PM spectrum was used to analyse the wave simulation, as shown in the formula below [11]:

Setting the test conditions

In order to ensure that the test conditions were consistent with the actual conditions, the wind speed was set to 1.56 m/s in the test, and the model rotor speed was set to 135 rpm based on the blade element momentum theory. Next, according to the wavelength selection principle for dangerous working conditions, the main scale length of the model was taken as the intermediate wavelength (2.1 m), and the arithmetic sequence was used to evaluate. The wave height was 6~14 cm with increments of 2 cm, as shown in Table 16.

Tab. 16. Wave parameters

Wave parameters	Cs_1	Cs_2	Cs_3	Cs_4	Cs_5
Wave length in test/m	1.26	1.68	2.1	2.52	2.94
Actual wavelength/m	63	84	105	126	147
Wave height in test/cm	6	8	10	12	14
Actual wave height/m	3	4	5	6	7
Wave direction/°	180	180	180	180	180

TEST RESULTS

The acceleration of the longitudinal motion of the motion sensor, the acceleration of the heave motion and the angle of the pitching motion were recorded using the motion sensor. In this paper, the influence of wave height and wavelength on the motion response of the model wind power platform is studied based on regular wave conditions. The test data after application of the scale conversion ratio are shown in Tables 17 to 20.

Tab. 17. Results of the model test

Serial number	Surge/m	Heave/m	Pitch/°
LC1	0.89	0.14	0.95
LC2	0.95	0.16	0.41
LC3	1.36	0.17	0.50
LC4	1.45	0.082	0.92
LC5	1.98	0.075	0.56
LC6	1.42	0.23	0.71
LC7	1.75	0.23	0.70
LC8	2.10	0.37	0.92
LC9	2.46	0.42	1.02

$$S(\omega, H_{\frac{1}{3}}, T_2, \theta) = \begin{cases} \frac{2}{\pi} 124 H_{\frac{1}{3}}^2 T_2^{-4} \omega^{-5} \exp\left(-\frac{496}{T_2^4 \omega^4}\right) \cos^2\theta & , -\frac{\pi}{2} \le \theta \le \frac{\pi}{2} \\ 0 & , \theta \text{ for other values} \end{cases} \tag{9}$$

where θ represents the angle between the combined wave and the main wave, in rad; $H_{\frac{1}{3}}$ represents the significant wave height, in m; T_2 represents the period of the wave crossing zero, in s; ω represents the angular frequency of the wave, in rad/s.

Tab. 18. Mooring tension at different wind speeds

Wind turbine rotation speed /rpm	Mooring tension/N		
	No.1 mooring line	No.2 mooring line	No.3 mooring line
95	0.29	0.1	0.8
135	0.31	0.15	0.85
175	0.33	0.21	0.87
215	0.30	0.19	0.88

Tab. 19. Mooring tension at different wavelengths

Wavelength /m	Mooring tension/N		
	No.1 mooring line	No.2 mooring line	No.3 mooring line
1.26	0.36	0.35	2.2
1.68	0.49	0.45	3.5
2.1	0.23	0.22	3.0
2.52	0.61	0.60	3.4
2.94	0.51	0.50	2.5

Tab. 20. Mooring tension at different wave heights

Wavelength /m	Mooring tension/N		
	No.1 mooring line	No.2 mooring line	No.3 mooring line
6	0.41	0.39	4
8	0.5	0.48	6
10	0.65	0.49	8
12	1	0.85	9
14	1.39	1.35	12

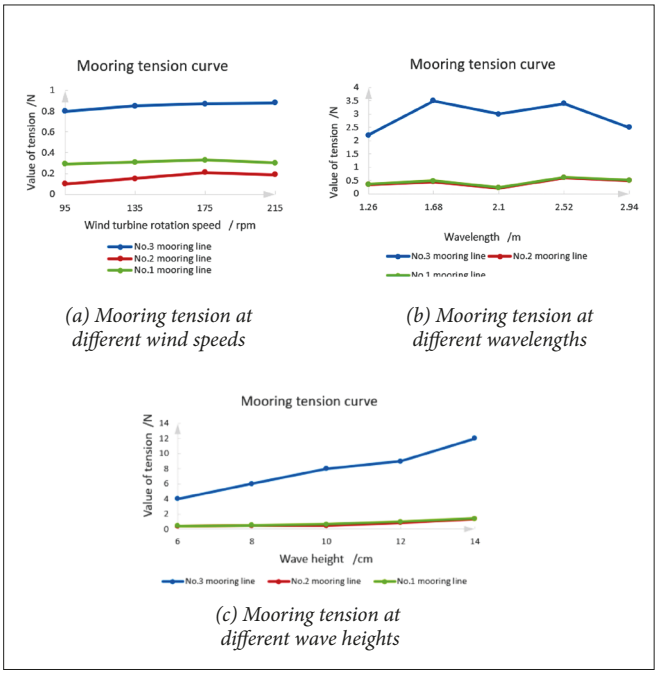

(a) Mooring tension at different wind speeds

(b) Mooring tension at different wavelengths

(c) Mooring tension at different wave heights

Fig. 9. Variation in mooring tension in the model test

Tab. 21. Results of numerical calculation and model test (invariant parameters: wave height 3 m, wave direction 180°)

Working conditions		LC1	LC2	LC3	LC4	LC5
Wavelength/m		63	84	105	126	147
Surge /m	Calculation	1	0.88	1.20	1.6	1.8
	Test data	0.89	0.95	1.36	1.45	1.98
	Data error%	11.00	7.95	13.33	9.38	10.00
Heave /m	Calculation	0.19	0.188	0.15	0.09	0.06
	Test data	0.14	0.16	0.17	0.082	0.075
	Data error%	26.32	14.89	13.33	8.89	25
Pitch /°	Calculation	0.9	0.36	0.4	0.8	0.7
	Test data	0.95	0.41	0.5	0.92	0.56
	Data error%	5.56	14	25	15	20

Tab. 22. Results of numerical calculation and model test (invariant parameters: wavelength 105 m, wave direction 180°)

Working conditions		LC3	LC6	LC7	LC8	LC9
Wave height/m		3	4	5	6	7
Surge /m	Calculation	1.20	1.54	1.92	2.31	2.7
	Test data	1.36	1.42	1.75	2.1	2.46
	Data error%	13.33	7.79	8.85	9.0	8.89
Heave /m	Calculation	0.15	0.2	0.25	0.3	0.35
	Test data	0.17	0.23	0.23	0.37	0.42
	Data error%	13.33	15.00	8.00	23	20.00
Pitch /°	Calculation	0.40	0.53	0.67	0.8	0.94
	Test data	0.50	0.71	0.7	0.92	1.02
	Data error%	25	16.98	4.48	15	8.51

Tab. 23. Comparison of mooring tension between numerical calculation and model test

Wavelength/m			1.26	1.68	2.1	2.52	2.94
Mooring tension /N	No.1 mooring line	Test results	0.36	0.49	0.23	0.61	0.51
		Numerical calculation	0.49	0.70	0.39	0.98	0.82
		Data error%	26.53	30	41.03	37.76	37.80
	No.2 mooring line	Test results	0.35	0.45	0.22	0.60	0.50
		Numerical calculation	0.45	0.69	0.38	0.81	0.65
		Data error%	22.22	34.78	42.11	25.93	23.08
	No.3 mooring line	Test results	2.2	3.5	3.0	3.4	2.5
		Numerical calculation	3.7	4.6	4.0	3.9	3.5
		Data error%	40.54	23.91	25	12.82	28.57

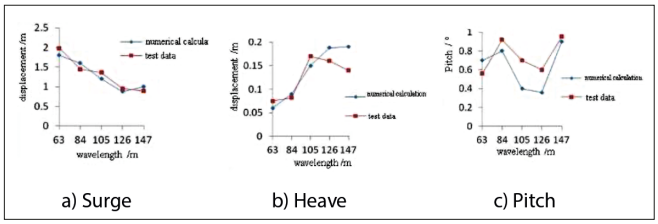

Fig. 10. Comparison of results from numerical calculation and model test (invariant parameters: wave height 3 m, wave direction 180°)

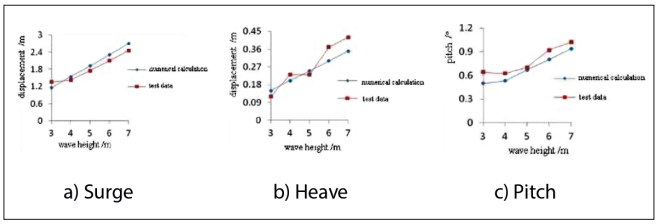

Fig. 11. Comparison of results from numerical calculation and model test (invariant parameters: wavelength 105 m, wave direction 180°)

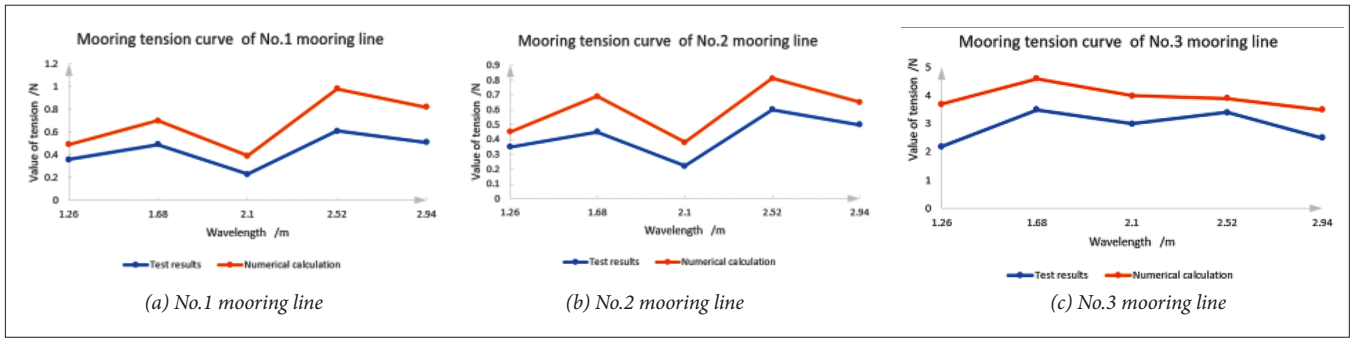

(a) No.1 mooring line *(b) No.2 mooring line* *(c) No.3 mooring line*

Fig. 12 Comparison of mooring tension for numerical calculation and model test

ANALYSIS AND COMPARISON

RESULTS

By comparing the results of the numerical calculation with those of the experimental test and analysing them, a comparison of the dynamic characteristics of the platform under the action of waves could be obtained, as shown in Tables 21–23 and Figs. 10–12.

ANALYSIS OF RESULTS

According to the analysis in Tables 21–23, it can be seen that the results from the test data and the numerical calculation are very similar, and the error between them is not large, at around 20%. The dynamic characteristics produced by the two methods for the wind power platform in waves are essentially the same. The results show that the overall calculation scheme for the floating wind power platform is feasible. The following laws can be obtained from Figs. 10 to 12:

(1) When the offshore wind speed is constant, the amplitude of the surge motion in the offshore motion response of the wind power platform is the largest, followed by the heave and pitch motion, and the various motion responses of the platform increase with the wave height.
(2) When the wave height is constant, the surge motion slows down with an increase in the wavelength. When the wavelength exceeds 126 m, the amplitude of the surge motion tends to be stable.
(3) When the wave height is constant, the heave and pitch motions of the platform first increase and then decrease with an increase in the wavelength. When the wavelength is close to the size of the platform, the motion reaches a peak.
(4) It can be seen from Figs. 8 and 11 that the amplitude of the mooring tension is largest when the motion of the platform is consistent with the direction of wave propagation, and reaches about eight times the mooring tension in the other two directions.
(5) The mooring tension increases with an increase in the wind speed, and first increases and then decreases with an increase in the wavelength. When the wavelength is close to the scale of the platform, the mooring tension has the largest value.

CONCLUSIONS

The following conclusions can be drawn from our analysis of the experimental and numerical results presented here.

(1) Of the six degrees of freedom in the movement of the wind power platform, the amplitude of the surge motion is the largest. Hence, in order to ensure the safety of offshore floating wind power platforms and continuous power generation, the longitudinal stability of platforms is paramount.
(2) The heave and pitch motions of the floating platform cannot be ignored. Before designing the layout of a wind farm, the sea conditions should be measured and investigated, and the wind power platform should not be placed in an area of the sea with a wavelength that is often close to the size of the platform.
(3) The floating wind farm should be built in an area of the sea where the surface is gentle and there will be no high waves.
(4) The wind at sea often causes waves from the same direction. When the wind direction and wave direction are the same, the wavelength is close to the scale of the platform length (in this paper, this specifically refers to the

length of the triangle formed by the foundation of three floating bodies), and the hydrodynamic characteristics of the platform will be most affected. In this case, in addition to the wave suppression measures on the platform, the anchor mooring tension in the same direction as the waves must be monitored and protected.

ACKNOWLEDGEMENTS

We acknowledge support from the National Natural Science Foundation of China (NSFC) (grant no. 51679217).

REFERENCES

1. A. Nematbakhsh, E.E. Bachynski, Z. Gao, and T. Moan (2015),Comparison of wave load effects on a TLP wind turbine by using computational fluid dynamics and potential flow theory approaches, *Applied Ocean Research*, vol. 53, no. 12, pp. 142–154.

2. C. Zhang(2017),Numerical calculation and experimental study of the motion response of multi-floating body offshore wind power platform, *ZheJiang Ocean University*.

3. E. Homayoun, H. Ghassemi, and H. Ghafari (2019), Power performance of the combined monopile wind turbine and floating buoy with heave-type wave energy converter, *Polish Marit. Res*., doi: 10.2478/pomr-2019-0051.

4. G. Abdalrahman, W. Melek, and F. Lien(2017), Pitch angle control for a small-scale Darrieus vertical axis wind turbine with straight blades (H-Type VAWT), *Renewable Energy*, vol. 114, Part B, no. 12, pp. 1353–1362.

5. M.Y. Liu(2016), Research on motion response characteristics of semisubmersible platform and optimization of design scheme, *Jiangsu University of Science and Technology*.

6. M.Y. Li(2013), Study on mooring system of floating offshore wind turbine platform, *Harbin Engineering University*, 2013.

7. P. Dymarski(2019), Design of jack-up platform for 6 MW wind turbine: Parametric analysis based dimensioning of platform legs, *Polish Marit. Res*., doi: 10.2478/pomr-2019-0038.

8. P. Dymarski, C. Dymarski, and E. Ciba(2020), Stability analysis of the floating offshore wind turbine support structure of cell spar type during its installation, *Polish Marit. Res*., doi: 10.2478/pomr-2019-0072.

9. W.X. Zhang and C. Lu(2016), Analysis of response of semi-submersible platform under freak wave," *Marine Technology*, vol. 333, no. 5, pp. 35–41.

10. X.M. Dong, Y.L. Cai, J.J. Li, and A.K. Song(2016), Study on TLP vortex induced motion at South China Sea," *China Offshore Platform*, vol. 31, no. 6, pp. 84–90.

11. Y.C. Liu, S.W. Li, Q. Yi, and D.Y. Chen(2016), Developments in semi-submersible floating foundations supporting wind turbines: A comprehensive review, *Renewable and Sustainable Energy Reviews*, vol. 60, no. 07 pp. 433–449.

CONTACT WITH THE AUTHORS

LI Junlai
e-mail: 11059979@qq.com

Wuhan University of Technology
No.1178, Heping Avenue
430063 Wuhan,Hubei
China